

# Learning a Phenotypic-Attribute Attentional Brain Connectivity Embedding for ADHD Classification using rs-fMRI

Ming-Shan Gao, Fu-Sheng Tsai, Chi-Chun Lee

**Abstract**—Automated diagnosis of Attention Deficit/Hyperactivity Disorder (ADHD) from brain’s functional imaging has gained more interest due to its high prevalence rates among children. While phenotypic information, such as age and gender, is known to be important in diagnosing ADHD and critically affects the representation derived from fMRI brain images, limited studies have integrated phenotypic information when learning discriminative embedding from brain imaging for such an automatic classification task. In this work, we propose to integrate age and gender attributes through attention mechanism that is jointly optimized when learning a brain connectivity embedding using convolutional variational autoencoder derived from resting state functional magnetic resonance imaging (rs-fMRI) data. Our proposed framework achieves a state-of-the-art average of 86.22% accuracy in ADHD vs. typical develop control (TDC) binary classification task evaluated across five public ADHD-200 competition datasets. Furthermore, our analysis points out that there are insufficient linked connections to the brain region of precuneus in the ADHD group.

## I. INTRODUCTION

Attention Deficit/Hyperactivity Disorder (ADHD) is one of the prevalent neurodevelopmental disorders among children with demonstrative abnormal mental characteristics. ADHD patients suffer from symptoms include impulsiveness, distractibility, and deficient concentration, which caused delayed mental, social relationship and adaptation development. It is often considered etiologically as a consequence of dietary, genetic and environmental factors [1]. Meanwhile, although the phenotypic information, such as age, gender and handedness, are not usually regarded as risk factors of ADHD, these factors play a critical role in the diagnostic process of one’s mental development [2]. Many research have also pointed out the impact of phenotypic attributes as a function on assessing ADHD’s mental ability. For example, B’alint et al. stated that males tend to demonstrate a larger difference of attention functioning comparing between ADHD and normal control group relative to females [3]; Chen et al. performed a logistic regression analysis on health insurance database and specified that relative age is a critical component for diagnosis and medication prescription for ADHD patients [4]

Being a neurodevelopmental disorder, researchers in neurophysiology have already extensively examined the relationship of brain’s dysfunction of ADHD subjects using BOLD (blood oxygen-level-dependent) signals in fMRI (functional

magnet resonance imaging) [5], especially resting state brain functions. The information about a subject’s phenotypic attributes is also shown to be important in performing machine learning based diagnosis of ADHD using rs-fMRI brain imaging. For example, Anderson et al. utilized a non-negative matrix factorization to embed phenotypic information in conducting differential diagnosis of ADHD [6]. With the recent advancement in artificial intelligence, several deep learning research have shown improved recognition rates of ADHD classification not only by advancing brain image representation learning [7] but also by including subject’s age and gender attribute as inputs to the learned classification networks. In fact, Riaz et al. has conducted a study in showing the importance of these phenotypic attributes by analyzing these features as inputs to a Elastic Net feature selection algorithm, and they demonstrated a substantial contribution of each personal attribute in classifying ADHD using rs-fMRI [8].

Most of previous computational studies, however, simply incorporate phenotypic attributes essentially as additional auxiliary inputs to the classifier without explicitly considering its impact when deriving a discriminative brain image neural representation for classification. In this work, we propose to learn a phenotypic-attribute, specifically age and gender, attentional brain connectivity embedding as a vectorized neural representation of the brain images gathered from rs-fMRI. Specifically, the embedding is learned from 90-ROI functional connectivity that is jointly optimized using an attention layer that is mechanistically controlled by age and gender attributes within a convolutional variational autoencoder architecture. We evaluate our proposed recognition framework for ADHD classification task on ADHD-200 global competition datasets [9]. The proposed framework achieves an overall average of 86.22% accuracy across five sites from different regions of the world. Further, we provide an analysis on the high attention brain connectivity regions to understand the key differences between typically develop control (TDC) and ADHD group.

## II. METHODOLOGY

### A. Database and Preprocessing

In this work, we conduct a binary classification task on ADHD-200 dataset [9], which was collected by the consortium of International Neuroimaging Datasharing Initiative (INDI). A total of 973 subjects from 8 individual sites had been aggregated. This dataset contained resting state fMRI, structural MRI, and phenotypic information. Also, each ADHD group was classified into 3 sub-types: Inattention,

MSG, FST, CCL are with Department of Electrical Engineering, National Tsing Hua University, Taiwan clee@ee.nthu.edu.tw

MSG, FST, CCL are with MOST Joint Research Center for AI Technology and All Vista Healthcare, Taiwan

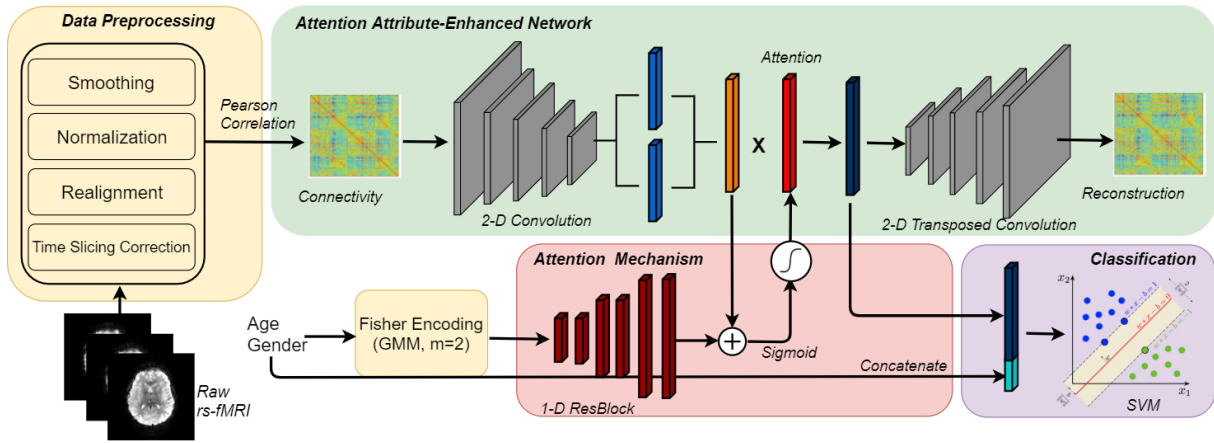


Fig. 1. Complete architecture for our proposed phenotypic-attribute attentional embedding that is jointly learned using age and gender within a convolutional variational autoencoder. We evaluate our classification framework in recognizing ADHD in the global ADHD-200 datasets.

TABLE I

SUMMARY OF DATA DISTRIBUTION ON TRAIN/TEST SPLIT IN EACH SITE.  
\*TDC: TYPICALLY DEVELOP CONTROL

Site	Training Set		Testing Set	
	TDC	ADHD	TDC	ADHD
NYU	98	117	12	29
Peking	116	78	27	24
OHSU	41	37	28	6
KKI	61	22	8	3
NeuroIMAGE	23	25	14	11

Hyperactivity and Combined. We exclude Bradley Hospital/Brown University from our experiment due to incomplete ADHD label. For the evaluation scheme, we utilize the same train/test set (listed in Table 1.) in “ADHD-200 Global Competition” in order to compare the performance fairly with the previous state-of-art approaches.

For data preprocessing, we obtained raw rs-fMRI data from NITRC’s website and performed all necessary steps using SPM12 [10], including slice timing correction, realignment, normalize and smoothing. For each site, we adjusted the parameter TR, TS and number of slices according to [9]. Meanwhile, we utilized SPM99 template bounding box and set voxel size to  $3 * 3 * 3 \text{ mm}^3$  in the normalization step. To decrease the impact of noise, we smoothed the former outcome by 5 mm FWHM Gaussian. In this work, we focus on the first 90 ROIs from AAL 116 atlas (Automated Anatomical Labeling) [11] to be our regions of interest.

### B. Phenotypic-Attribute Attentional Embedding

Figure 1 depicts our overall classification scheme. The attention attribute-enhanced network (AAEN) is used to derive our phenotypic-attribute attentional brain connectivity embedding. This latent representation is concatenated with age and gender attributes as final feature vector to be fed into a support vector machine (SVM) for ADHD classification.

1) *Brain Connectivity Matrix*: In order to transform the original time series of BOLD signals to characterize brain functions, we compute functional connectivity of each subject on his/her recorded rs-fMRI data. Specifically, we compute the Pearson’s correlation on voxel mean between pairs

of ROIs which results in a  $90 \times 90$  symmetric matrix. The matrix’s diagonal element is 1 and remain element has values ranging from -1 to 1 indicating the degree of connectivity value for each pair of ROI (representing inter-brain region functional connectivity).

2) *Convolutional Variational Autoencoder*: Convolutional Variational Autoencoder (CVAE) [14] has been used as a powerful unsupervised generative model learning approach across a variety of machine learning tasks (especially in the domain of computer vision). Recent work [15] has started to use CVAE models as a representation learning approach to derive latent representation of rs-fMRI. In this work, we also use CVAE as our basic building block in learning the latent connectivity embedding from resting state fMRI data.

3) *Phenotypic-Attribute Attention Mechanism*: In this work, our aim is to learn a phenotypic-attribute attentional latent representation of rs-fMRI as characterized using brain connectivity matrix. In specifics, age and gender are the two attributes to be integrated in this task. We first compute a Fisher representation [16] using Gaussian mixture number equals to 2 as a vectorized representation of phenotype information. This vector is first passed through a 7-layers 1D residual blocks to obtain a deep phenotype representation, and by taking the sigmoid function of the summation between the latent vector of CVAE with this deep phenotype vector, we can derive attention weights that are multiplied back to the CVAE latent vector to generate our *phenotypic-attribute attentional brain connectivity embedding*:

$$W_{Att} = \text{Sigmoid}(L_{i,pho.} + L_{j,cvae}) \quad (1)$$

where,

$$L_{i,pho.} = \text{ReLU}(\text{ReLU}(Wx + b) + x) \quad (2)$$

$$L_{j,cvae} = \mu(X) + \Sigma^{1/2}(X) \cdot \epsilon \quad (3)$$

$W_{Att}$  is the final attention weight we used.  $L_{j,cvae}$  denotes CVAE’s latent reparameterized by variational mean vector  $\mu(X)$  and variance vector  $\Sigma^{1/2}(X)$ .  $L_{i,pho.}$  denotes the phenotype representation outputted from 1D residual blocks.

TABLE II

A COMPARISON OF RECOGNITION RESULTS INCLUDING OUR PROPOSED METHOD AND THE COMPARISON MODELS. ACCURACY IS USED AS OUR METRIC.

<i>Comparison Model</i>	<i>NYU</i>			<i>Peking</i>			<i>KKI</i>			<i>OHSU</i>			<i>NeuroIMAGE</i>		
	Acc.	Sens.	Spec.	Acc.	Sens.	Spec.	Acc.	Sens.	Spec.	Acc.	Sens.	Spec.	Acc.	Sens.	Spec.
<i>CVAE</i>	72.19	75.17	65.00	69.41	68.33	70.37	90.90	86.66	92.50	81.17	68.33	70.30	76.00	78.18	74.28
<i>CVAE<sub>pho</sub></i>	71.54	72.41	69.44	74.50	63.88	83.95	87.87	61.16	95.83	80.39	83.33	79.76	89.33	87.87	90.47
<i>CVAE-Merge<sub>pho</sub></i>	69.10	71.49	58.31	72.28	64.72	76.29	83.63	78.57	91.66	73.13	60.00	73.80	97.60	82.42	92.85
<i>CVAE-DNN<sub>pho</sub></i>	75.60	87.33	32.22	75.81	65.36	80.07	87.87	88.88	87.50	74.50	61.11	77.38	96.00	87.27	88.57
<i>Proposed Method</i>	<b>76.42</b>	<b>80.45</b>	<b>66.66</b>	<b>78.43</b>	<b>72.22</b>	<b>83.95</b>	<b>94.54</b>	<b>93.33</b>	<b>95.00</b>	<b>83.33</b>	<b>44.45</b>	<b>89.28</b>	<b>98.40</b>	<b>98.18</b>	<b>97.14</b>

TABLE III

A COMPARISON OF RECOGNITION RESULT TO PREVIOUS RESEARCH.

<i>Approaches</i>	<i>NYU</i>	<i>Peking</i>	<i>KKI</i>	<i>NeuroIMAGE</i>
<i>Zou et al. [12]</i>	70.50	62.95	72.82	-
<i>Riaz et al. [8]</i>	60.90	64.70	81.80	44.00
<i>S. Itani et al. [13]</i>	68.30	<b>82.40</b>	-	-
<i>Miao et al. [7]</i>	70.73	68.63	81.82	76.00
<i>Proposed Method</i>	<b>76.42</b>	78.43	<b>94.54</b>	<b>98.40</b>

Our final classification is done by training a linear SVM on latent vector derived from attention attribute-enhanced network concatenated with raw phenotype attribute values.

### III. EXPERIMENTAL SETUP AND RESULT

In our experiment, we follow the train-test division of ADHD-200 global competition and evaluate our model using the exactly same architecture on five separate data collection sites. This evaluation scheme is done by following closely with the past literature on the same dataset, which measures classification accuracy; we further present sensitivity and specificity for completeness. All of the network optimization, feature selection, and hyperparameter tuning are done strictly within the training set.

#### A. Experiment Setup

We carry out TDC versus ADHD classification task with hyper-parameters settings set to the follows: learning rate: 0.0003, epochs 2000, Adam optimizer. Based on the number of samples in each site, we adaptively choose the batch size to be 64 for NYU and Peking, and 32 for the remaining three sites (KKI, OHSU, NeuroIMAGE). We repeat our framework five times and report average of the highest accuracy to demonstrate a more robust performance metric.

#### B. Comparison Models

In this section, we compare our framework with the following approaches including a variant usage of integrating phenotypic attributes in rs-fMRI based ADHD classification:

- CVAE, CVAE<sub>pho</sub>: This model is considered as a baseline by directly utilizing the CVAE’s latent for recognition. The subscript “pho” represent a direct concatenation of raw phenotypic attributes as input to SVM.
- CVAE-Merge<sub>pho</sub>: This model takes raw phenotypic attributes and concatenate it to CVAE’s encoded latent to serve as an additional information during the learning of the decoding portion of CVAE.
- CVAE-DNN<sub>pho</sub>: Apart from directly combining phenotypic attribute like CVAE-Merge, this model passes these attributes through a DNN containing 3 fully-connected layers of size [2-4-4-8] and a sigmoid function before merging into the CVAE’s latent.

- AANE: Our proposed method (see section II.B)

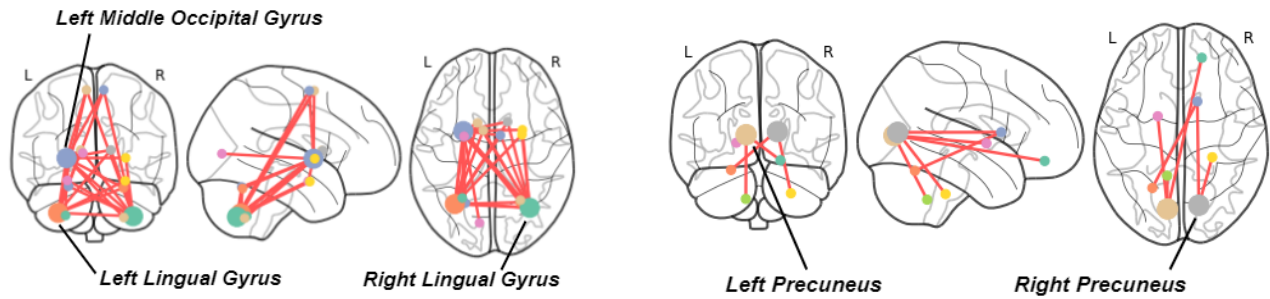
#### C. Experiment Results

Table 2 summarizes our complete experiment results. In general, by performing attention reweighing approach, which considers age and gender attributes in learning brain connectivity network embedding, provides a more discriminative brain’s rs-fMRI representation for ADHD classification. Our proposed method achieves the best performances in all five sites. Especially in KKI and OHSU, our framework achieves recognition accuracy up to 94.54% and 83.33%, which improves the second best CVAE-DNN<sub>pho</sub> model by 6.67% and 8.83% relative. When comparing with all other baseline models, we observe a clear superior discriminative power of our proposed brain rs-fMRI representation.

Furthermore, table 3 summaries the recognition accuracy when comparing our proposed method with other recently-published works on the same dataset using the exact same train-test split. Aside from one site, our proposed method achieves the best performance in differentiating ADHD and TDC known to date. The only lower performance occurs when comparing to the framework proposed by Itani et al. for data from the Peking site. Itani et al. also integrates phenotypic attributes into their framework but through the use of a decision tree approach. We will further investigate and compare our neural embedding method versus decision tree clustering method in handling phenotype information. However, it is promising to see that our proposed framework demonstrates almost a consistently higher performance by using neural-embedding based method in integrating phenotypic attributes when learning brain connectivity representation in ADHD versus TDC classification with rs-fMRI.

#### D. Connectivity Visualization and Analyses

A key feature of our method is that due to it being an attention based method, we can further perform analysis by reconstructing those high attention weighted latent dimensions using the learned decoding layer. For each site, we select top 10 attention weights to perform connectivity matrix reconstruction and only maintain the top 10% connectivity edges as the most contributing functional connection within the brain in differentiating those TDC from ADHD. In Figure 2 (a), we plot top 3 regional connections exists in both TDC and ADHD group across all five sites, and in Figure 2 (b), we plot those connectivity exists in TDC but not in ADHD. From Figure 2 (b), we observe several key connections missing in the ADHD group as compared to the TDC group. Interestingly, the key region missing from the ADHD group’s



(a) Visualization of connectivity in both ADHD and TDC groups.

(b) Visualization of deficient connectivity in ADHD groups.

Fig. 2. (a) Top connectivity visualization from three angles, the top 3 most contributing brain regions in both groups (TDC, ADHD) are left middle occipital gyrus, left and right lingual gyrus respectively. (b) The edges show the connection exists in TDC not in ADHD, the deficient connectivity of ADHD groups comes from missing connection of precuneus region to angular gyrus, inferior parietal, superior parietal gyrus and median cingulate.

connectivity is precuneus, i.e., we see a missing link from precuneus to angular gyrus, inferior parietal, superior parietal gyrus and median cingulate. This result corroborates with many past research in neuroscience. Precuneus has been recognized to be involved with consciousness, self-awareness and episodic memory [17]. Within the Theory of Mind (ToM) and Execution Function (EF) studies, many works have indicated that the deficiency of the mental ability in ADHD [18] is associated with the bilateral from precuneus to angular gyrus [19] (as similarly found in our observation). In fact, angular gyrus has also been regarded as region for attention, spatial cognition and verbal working memory [20], which is also known to have insufficient activation in subjects with ADHD [21] and is observed in our analysis.

#### IV. CONCLUSIONS

In this work, we present a computational rs-fMRI neural embedding framework that learns a phenotypic-attribute based attention re-weighting mechanism for ADHD classification task. The AAEN architecture models age-gender attributes to enhance the modeling capacity of the latent feature representation derived from convolutional variational autoencoder. By using this novel representation, our recognition framework evaluated on the global ADHD-200 dataset outperforms almost all of the existing state-of-the-art approaches across five sites. Our results demonstrate that the proposed framework not only enhance the discriminative power but also is capable at pointing out affected brain regions functionally by reconstructing the high attention latent dimensions. To our knowledge, this is the first study that performs joint neural embedding in learning the brain connectivity representation together with personal phenotype attributes, which demonstrates a consistent state-of-the-art modeling power across different datasets of ADHD rs-fMRI. In our future work, we will devise data augmentation strategy on top of this personal phenotypic generative CVAE model to handle situations where large quantity of data can be hard to obtain. Having an automated classification instrument for ADHD would hopefully lead to a more precise diagnosis method and further improve treatment decisions.

#### REFERENCES

[1] National Collaborating Centre for Mental Health, "Attention deficit hyperactivity disorder: diagnosis and management of ADHD in children, young people and adults." British Psychological Society, 2018.

[2] Gaub, M. and Carlson, C. L., "Gender differences in ADHD: a meta-analysis and critical review". *Journal of the American Academy of Child and Adolescent Psychiatry*, 36(8), 1136-1139, 1997.

[3] S Balint, P Czobor, S Komlosi and et al., "Attention deficit hyperactivity disorder (ADHD): gender-and age-related differences in neurocognition." *Psychological medicine* 39.8, 1337-1345, 2009.

[4] Chen, Mu-Hong and et al., "Influence of relative age on diagnosis and treatment of attention-deficit hyperactivity disorder in Taiwanese children." *The Journal of pediatrics* 172, 162-167, 2016.

[5] Krain, Amy L., and F. Xavier Castellanos, "Brain development and ADHD." *Clinical psychology review* 26.4, 433-444, 2006.

[6] Anderson, A., Douglas, P. K., Kerr, W. T. and et al., "Non-negative matrix factorization of multimodal MRI, fMRI and phenotypic data reveals differential changes in default mode subnetworks in ADHD." *NeuroImage*, 102, 207-219, 2014.

[7] Miao, B., Zhang, L. L., Guan, J. L., and et al., "Classification of ADHD individuals and neurotypicals using reliable RELIEF: A resting-state study." *IEEE Access*, 7, 2019.

[8] Riaz, A., Asad, M., Alonso, E. and Slabaugh, G., "Fusion of fMRI and non-imaging data for ADHD classification." *Computerized Medical Imaging and Graphics*, 65, 2018.

[9] Bellec, P., Chu, C., Chouinard-Decorte, F. and et al., "The neuro bureau adhd-200 preprocessed repository." *Neuroimage*, 144, 2017.

[10] Penny, W. D., Friston, K. J. and et al., "Statistical parametric mapping: the analysis of functional brain images." Elsevier, 2011.

[11] Tzourio-Mazoyer, N., Landeau, B., Papathanassiou, D. and et al., "Automated anatomical labeling of activations in SPM using a macroscopic anatomical parcellation of the MNI MRI single-subject brain." *Neuroimage*, 15(1), 273-289, 2002.

[12] Zou, L., Zheng, J., Miao, C. and et al., "3D CNN based automatic diagnosis of attention deficit hyperactivity disorder using functional and structural MRI." *IEEE Access*, 5, 2017.

[13] Itani, S., Lecron, F., and Fortemps, P., "A multi-level classification framework for multi-site medical data: Application to the ADHD-200 collection. *Expert Systems with Applications*," 91, 36-45, 2018.

[14] Kingma, D. P. and Welling, M., "Auto-encoding variational bayes." *arXiv preprint*, 2013.

[15] Choi, H., "Functional connectivity patterns of autism spectrum disorder identified by deep feature learning." *arXiv preprint*, 2017.

[16] Perronnin, F. and Dance, C., "Fisher kernels on visual vocabularies for image categorization". *IEEE conference on computer vision and pattern recognition*, 2007.

[17] Cavanna, A. E. and Trimble, M. R., "The precuneus: a review of its functional anatomy and behavioural correlates." *Brain*, 129, 2006.

[18] Caillies, S., Bertot, V. and et al., "Social cognition in ADHD: Irony understanding and recursive theory of mind." *Research in developmental disabilities*, 35(11), 3191-3198, 2014.

[19] Uddin, L. Q., Kelly, A. C., Biswal, B. B. and et al., "Network homogeneity reveals decreased integrity of default-mode network in ADHD." *Journal of neuroscience methods*, 169(1), 249-254, 2008.

[20] Seghier, M. L., "The angular gyrus: multiple functions and multiple subdivisions." *The Neuroscientist*, 19(1), 43-61, 2013.

[21] Burgess, G. C., Depue, B. E., and et al., "Attentional control activation relates to working memory in attention-deficit/hyperactivity disorder." *Biological psychiatry*, 67(7), 632-640, 2010.